Ohmura et al. *NPG Asia Materials* (2023) 15:2
https://doi.org/10.1038/s41427-022-00454-9

NPG Asia Materials

ARTICLE Open Access

Squid/synthetic polymer double-network gel: elaborated anisotropy and outstanding fracture toughness characteristics

Shou Ohmura[1], Tasuku Nakajima[2,3], Masahiro Yoshida[1] and Jian Ping Gong[2,3]

Abstract

The hierarchical anisotropy of a biotissue plays an essential role in its elaborate functions. To mimic the anisotropy-based functions of biotissues, soft and wet synthetic hydrogels with sophisticated biotissue-like anisotropy have been extensively explored. However, most existing synthetically manufactured anisotropic hydrogels exhibit fundamental anisotropy and poor mechanical toughness characteristics. In this paper, natural/synthetic hybrid double-network (DN) hydrogels with hierarchical anisotropy and high toughness characteristics are reported. These DN gels are prepared directly by using a squid mantle as an anisotropic soft bioproduct for the primary network and polyacrylamide (PAAm) as a synthetic polymer for the secondary network. The obtained squid/PAAm DN gel maintains the complex orientation of the muscle fibers of the squid mantle and exhibits anisotropic, enhanced mechanical properties and excellent fracture resistance due to its unique composite structure. This hybrid strategy provides a general method for preparing hydrogels with elaborated anisotropy and determining functions derived from the anisotropy.

Introduction

The anisotropy characteristics of biotissues are essential for the elaborate functions and activities of organisms[1]. For example, muscles enable directional movements due to unidirectional and hierarchical muscle fibers[2]. Nacres and bones are extremely tough anisotropic composites that can sustain heavy impact[3]. Vascular bundles enable the directional transportation of nutrients in plants[4]. The complex metabolic pathways of organisms synthesize these tissues with three-dimensional (3D) and hierarchical anisotropy characteristics through a process that consumes little energy. However, hydrogels are materials that contain water inside the polymer network. Hydrogels have attracted significant attention as materials that can potentially mimic various functions of soft biotissues because their soft and wet properties are similar. For example, hydrogel-based actuating devices[5], tough hydrogels[6–10], and mass transportation actions by hydrogels have been developed thus far[11]. However, although most biotissues exhibit distinct functions due to their anisotropy characteristics, the structures, properties, and functions of typical hydrogels remain isotropic. Various attempts to introduce anisotropy into hydrogels have been made to reproduce the distinct functions of anisotropic biotissues[12]. Monodomain liquid crystalline hydrogels[13,14] and hydrogels made from the directional assemblies of biopolymers have been prepared using molecular-scale approaches[15,16]. Moreover, hydrogels with aligned voids[17], hydrogels with oriented nanofillers trapped in the network[18], and 3D-printed hydrogels have been prepared through mesoscale approaches[19]. These synthetically manufactured anisotropic hydrogels exhibit a certain level of anisotropic properties; however, most of them only have very fundamental anisotropies, such as uniform uniaxial or biaxial orientations, which are dissimilar to the elaborate anisotropy of organisms.

Correspondence: Tasuku Nakajima (tasuku@sci.hokudai.ac.jp) or Jian Ping Gong (gong@sci.hokudai.ac.jp)
[1]Graduate School of Life Science, Hokkaido University, Sapporo, Hokkaido 001-0021, Japan
[2]Faculty of Advanced Life Science, Hokkaido University, Sapporo, Hokkaido 001-0021, Japan
Full list of author information is available at the end of the article

Moreover, mesoscale approaches consume a large amount of energy to construct anisotropy, such as a strong magnetic field for unidirectional nanofiller orientation[17]. Furthermore, most synthetic hydrogels comprising nonorganized polymer networks have poor mechanical properties, limiting their applicability as structural materials. As shown above, mimicking the elaborate functions of biotissues using synthetic hydrogels remains challenging.

To address this issue, in this study, we propose a natural/synthetic hybrid double-network (DN) hydrogel prepared by utilizing bioderived products that already have anisotropic structures as their primary networks. DN hydrogels are tough and strong interpenetrating network hydrogels obtained from stiff and brittle primary networks and soft and flexible secondary networks[7,8]. Due to the large stiffness value, the initial mechanical responses of DN gels are dominated by their primary network[8]. While the sole primary network typically possesses low mechanical strength due to the stress concentration at the defect and the subsequent crack propagation, the flexible secondary network suppresses the stress concentration in the primary network; these phenomena significantly improve the fracture resistance of the DN gel[8]. As a result, DN gels exhibit large compressive fracture strengths comparable to those of human knee cartilage[7,8]. A wide variety of polymer species can be used as the primary network for DN gels. While covalently cross-linked isotropic polymer networks were used in the original report[7], noncovalently cross-linked natural polymer networks[20,21], anisotropic liquid crystalline gels[22,23], and jellyfish have been adopted as the primary networks of DN gels[24]. The mechanical characteristics and functions of DN gels vary widely depending on the primary network species. The isotropic primary network leads to the isotropic characteristics of the DN gels. For the anisotropic primary network, the resulting DN gels are mechanically anisotropic[21–23]. Moreover, DN gels generally maintain the chemical or physical functions of their parent networks[25]. If DN gels are synthesized with highly anisotropic bioderived products as their primary components, the obtained DN gels are expected to have high strengths and elaborative anisotropic functions of the primary network.

In this study, as a proof-of-concept of our strategy, we report such a DN gel utilizing the mantle of the squid (*Ommastrephes bartramii*) as an anisotropic bioproduct. Squid mantles are soft and wet muscular tissues that provide fast locomotion to squids with jet propulsion[26,27]. A mantle expands to take water inside and then strongly contracts to shoot water as a jet. To realize this powerful movement, the squid mantle contains two types of anisotropic muscles with connective tissues, as shown in Fig. 1a[26–29]. The circular muscle, with muscle fibers that run circumferentially to the mantle, is a major component contributing to mantle contraction. The radial muscle, oriented perpendicular to the circular muscle, is a minor component contributing to mantle re-expansion. Since squid mantle is mainly composed of muscle fibers and connective tissues that noncovalently bind muscle fibers, in this paper, we state the squid mantle as a physically cross-linked gel/network. The mechanical properties of the mantle are anisotropic mainly due to the structural anisotropy of the circular muscle[30–32]. The fresh squid mantle exhibits a higher tensile strength when stretched parallel to the circular muscle than when stretched perpendicularly[30,31]. The rupture energy of the fresh squid mantle is higher when broken parallel to the circular muscle than when broken perpendicularly[32]. When the mantle is cooked by heating, the relationships between the orientation of the circular muscle and the mechanical properties are reversed due to the heat-induced damage to the structures[30–32].

We use a squid mantle as the primary network and synthesize a polyacrylamide (PAAm) network inside the mantle as the secondary network to create a squid/PAAm DN gel. We demonstrate anisotropic and significant fracture toughness characteristics of the squid/PAAm DN gel due to the sophisticated anisotropy.

Materials and methods

Materials

Frozen squid mantles (*Ommastrephes bartramii*) were purchased from Tsukiji Gyogun Dream Island Co. Ltd., Japan. Acrylamide (AAm), *N*,*N*-dimethylacrylamide (DMAAm), *N*,*N*'-methylenebis (acrylamide) (MBAA), ammonium peroxydisulfate (APS), and sea sand (425–850 μm/20–35 mesh) were purchased from FUJIFILM Wako Pure Chemical Corporation Inc., Japan. Osmium tetroxide 1% aqueous solution was purchased from Nissin EM Co. Ltd., Japan. All chemicals were used as received without further treatment.

Synthesis of squid/PAAm DN gels

The squid mantles were defrosted at ambient temperature and sliced into thin rectangular shapes. The obtained slices were immersed in aqueous solutions containing AAm (4 or 6 M), MBAA (0.1 mol% to monomer) as a cross-linker, and APS (0.1 mol% to monomer) as an initiator for at least 3 d. Then, these slices were placed in a 65 °C oven for 10 h to initiate the thermal polymerization of AAm and MBAA in the squid slices. The squid/PDMAAm gel was prepared with the same procedure while using DMAAm instead of AAm. For reference PAAm single-network gels, AAm (6 M), MBAA (0.1 mol% to monomer) as a cross-linker and APS (0.1 mol% to monomer) as an initiator were dissolved in pure water. The solutions were poured into rectangular glass molds and thermally polymerized at 65 °C for 10 h in an oven.

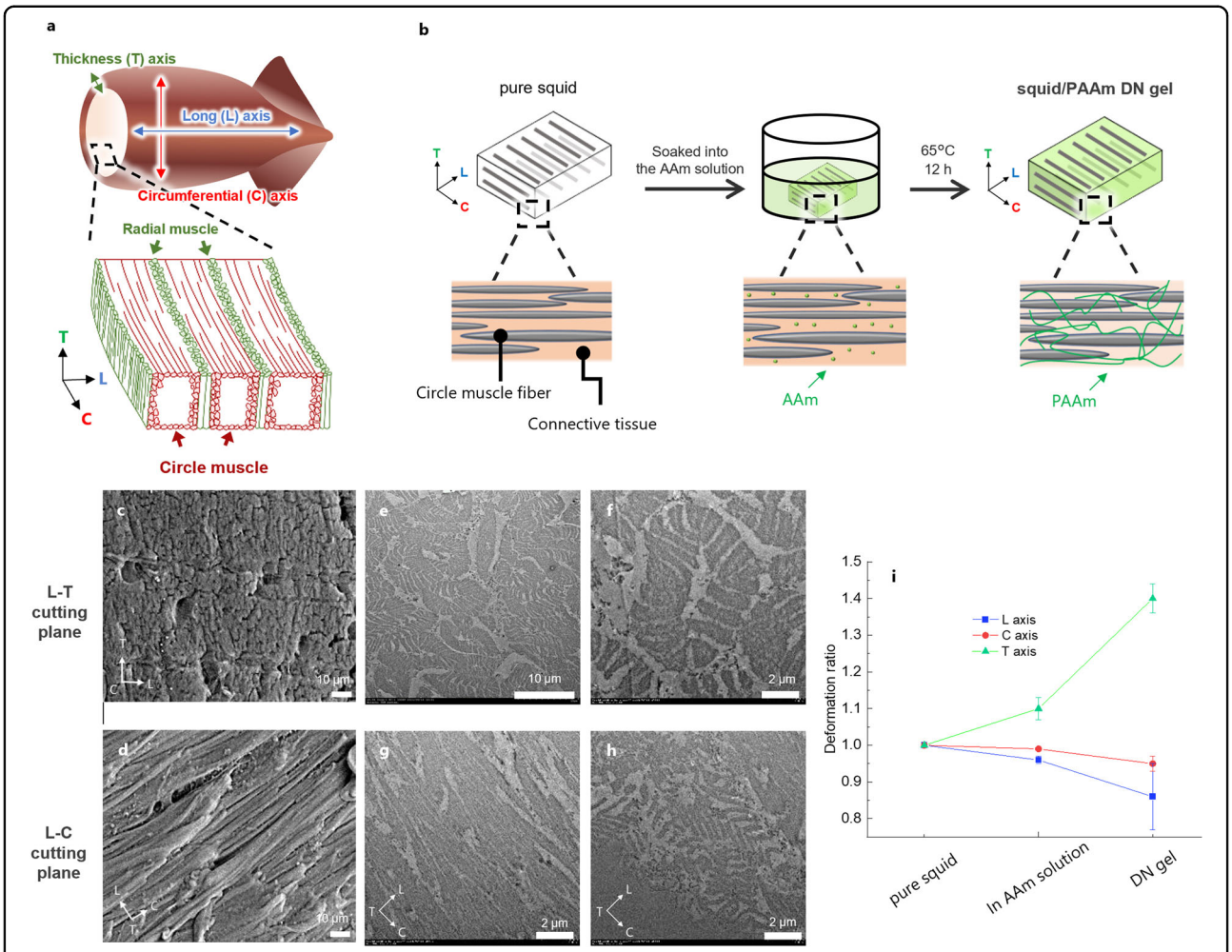

Fig. 1 Anisotropic structures of the squid/PAAm DN gels. a Macroscopic and microscopic illustrations of the structures of squid mantles. **b** Preparation process of the squid/PAAm DN gel from pure squid. LV–SEM images of the **c** L–T and **d** L–C cutting surfaces of the squid/PAAm-6 DN gel. TEM images of the (**e, f**) L–T and (**g, h**) L–C cutting surfaces of the squid/PDMAAm-6 DN gels. Muscle fibers in circular muscles were selectively stained with osmium tetroxide. **i** Deformation ratio of each axis of the squid upon preparing the squid/PAAm-6 DN gel. Data are represented as the mean ± SD with $n = 3$.

For heated squids, the cut rectangular squids were put in a glass mold and heated at 65 °C for 10 h in an oven. After the processes, the as-prepared samples were packed into a plastic bag to prevent drying without soaking in water and stored at 4 °C. The as-prepared samples were subjected to the following measurements within one week of preparation. For the degradation resistance measurements, the bags containing the samples were left at 4 °C for two months or soaked in 90 °C hot water for 1 h.

Low-vacuum scanning electron microscopy (LV–SEM) analysis

The cut and fractured surfaces of the samples were characterized by a scanning electron microscope in low-vacuum mode (JSM-6010LA, JEOL Ltd., Japan). A razor blade was used to create the cut surface. The gels were observed without drying, ion sputtering, or other treatments under low-vacuum conditions, with an acceleration voltage of 10 kV.

Transmission electron microscopy (TEM) analysis

TEM analysis was performed to observe the morphologies of the squid/PDMAAm DN hydrogels stained with H-7650 (Hitachi High-Tech *Co.*, Japan)[33]. The hydrogels were frozen in liquid nitrogen; the water in the frozen hydrogels was substituted with ethanol and then acrylic resin (London Resin white, medium) in the chamber of an automatic freeze substitution system (EM AFS2, Leica Microsystems, Germany). Then, 100-nm-thick resin-cured specimens were cut using an ultramicrotome knife (EM UC7i, Leica Microsystems, Germany) and placed on a carbon-supported copper

mesh grid. The e-gun had an acceleration voltage of 100 kV.

Water content analysis

The water contents of the pure squid and squid/PAAm DN gel were measured by a moisture balance (MOC-120H, Shimadzu *Co*., Japan). The samples were covered with sea sand in a moisture balance and heated at 120 °C until completely dry. The water contents of the samples were analyzed by $(W_w - W_d)/W_w$, where W_w and W_d were the weights of the wet sample and the dried sample, respectively.

ATR–FTIR analysis

The pure squid, squid/PAAm DN gel, and PAAm gel were analyzed with attenuated total reflectance Fourier transform infrared spectroscopy (ATR–FTIR). The cut surfaces of the samples were analyzed with an FTIR 6600 equipped with an IRT-5200 (JASCO Co., Japan). A razor blade was used to create the cut surface. Each spectrum was recorded in are range of 4000–400 cm^{-1} from an average of 32 scans at a resolution of 2 cm^{-1}.

Tensile and cycle tensile tests

Uniaxial tensile tests were conducted using an Instron 5965 commercial tensile tester (Instron *Co*., USA). The samples were cut into dumbbell shapes (12 mm gauge length and 2 mm width). The tensile velocity was fixed at 100 mm/min, which corresponded to a strain rate of 0.14 s^{-1}. The nominal stress, σ, was defined as the retraction force divided by the initial cross-sectional area of the sample. The nominal strain, ε, was defined as the displacement of the sample divided by its original length. The fracture strain was defined as ε at the fracture point. The maximum stress was defined as the maximum σ during the test.

Cyclic tensile measurements were performed on the same specimens using an Instron 5965. The samples were first elongated to a certain target strain and then immediately unloaded. After the jig head returned to its initial position, it was immediately elongated to a larger target strain and unloaded. The tests were repeated until the specimens fractured. The loading and unloading velocities were fixed at 100 mm/min.

Fracture tests

Two types of fracture tests were conducted on the squid/PAAm DN gels and corresponding pure squid and heated squid to evaluate their anisotropic fracture toughness values[34]. For the single-edge notch test, samples were cut into rectangular shapes (70 mm gauge length and 7 mm width) with or without an initial notch (notch length $c = 2$ mm) on the edge of the long axes of the samples. The samples were then uniaxially stretched at constant velocities of 100 mm/min using an Instron 5965 commercial tensile tester. For the trouser tear test, samples were cut into trouser shapes (pure squid and heated squid: 70 mm in length with legs 30 mm in initial length and 15 mm in width; squid/PAAm DN gel: 50 mm in length with legs 20 mm in initial length and 7.5 mm in width). Tearing was performed by pulling one leg of the sample at a constant velocity of 500 mm/min using an Instron 5965 to induce crack growth.

Notch introduction tests

Notch introduction tests of the squid/PAAm DN gels were conducted to demonstrate their high fracture resistance characteristics. We hung rectangular DN gel (70-mm length and 7-mm width) with 500 g weight and then imposed the crack on the C–T plane or L–T plane with scissors; the sample size was the same as the single-edge-notch test.

Statistical analysis

The Student's *t*-test was used in the Supplementary information to check for the statistical significance values of different groups, and a two-sided $p < 0.05$ was considered significant.

Results

Preparation of the squid/PAAm composite

The defrosted squid mantle was immersed in the second network precursor solution. The secondary PAAm network was then synthesized from the monomer and cross-linker in the presence of a squid mantle to prepare squid/PAAm-*X* gels by thermal polymerization at 65 °C, where *X* is the molar feed concentration of AAm for polymerization (Fig. 1b). For the squid/PAAm-6 DN gel, the formation of the squid/PAAm composite was confirmed by Fourier transform infrared spectroscopy (Supplementary Fig. 1a), and its composition ratio was estimated to be approximately 69.2 wt.% water, 18.0 wt.% PAAm, and 12.8 wt.% solids derived from squid (Supplementary Note 1). PAAm was uniformly distributed in the squid/PAAm DN gel (Supplementary Fig. 1b, c), suggesting the sufficient penetration of AAm monomers in the mantle.

Hereafter, the long (L), circumferential (C), and thickness (T) axes shown in Fig. 1a were used to describe the directions of the squid samples. The L–T and L–C planes of the as-prepared squid/PAAm-6 DN gels were cut using a razor blade and observed by low-vacuum scanning electron microscopy (LV–SEM). LV–SEM was suitable for the observation of wet samples because the wet samples could be measured without any pretreatment, such as freeze-drying, which could introduce artifacts in observed images. In the L–T cross-sectional image shown in Fig. 1c, the cross-sections of the fibers were observed. In the L–C cross-sectional images shown in Fig. 1d, unidirectionally

oriented fibers along the C-axis were observed. These fibers corresponded to circular muscle fibers running along the C-axis[27]. Transmission electron microscopy (TEM) was used to observe the structures of the DN gels with higher magnification levels. For TEM analysis, a secondary network of poly (*N*,*N*-dimethylacrylamide) (PDMAAm) instead of PAAm was adopted due to the high affinity of PDMAAm to ethanol, making the DN gels suitable for resin-embedding treatment for TEM observation[33]. Figure 1e–h shows TEM images of the squid/PDMAAm DN gels after their water was replaced with resin. Due to the high resolution, an elliptical leaf-like structure of the circular muscle fibers was observed in the L–T cross-sectional images (Figs. 1e and 1f). In the L–C cross-sectional images shown in Figs. 1g and 1h, in addition to the parallel orientation circular muscle fibers, a cross-section of a radial muscle oriented along the T-axis was observed, as reported in a previous study[26]. The radial muscle of a pure squid exhibited an elliptical shape similar to that of a circular muscle, while the elliptical structure shown in Fig. 1h was slightly obscured. These electron microscopic images indicated that the structures of the muscles of the squid mantle were preserved in the DN gels.

Deformations of the squid along the L-, C-, and T-axes upon the preparation of the squid/PAAm-6 DN gel were investigated. As shown in Fig. 1i, the squid finally shrank by 5% along the C-axis and 14% along the L-axis; however, along the T-axis, the squid thickened by 40%. Such transverse and longitudinal contractions and thickness increases of a squid upon heating were previously reported[31]. Squid muscle fibers composed of water-insoluble proteins maintain their structure after heat or chemical treatment[35,36]. However, the connective tissue of squid binding the muscle fibers mainly consisted of water-soluble collagen and partially gelatinized and dissolved after heat or chemical treatment[32,35,36]. This phenomenon implied that the observed deformations of the squid occurred mainly due to damage to the connective tissue caused by chemical (immersion in the precursor solution) and heat (thermal polymerization at 65 °C) stimuli. The slight collapse of the radial muscle observed using TEM (Fig. 1h) was explained by the deterioration of the connective tissue.

Anisotropic tensile properties of the squid/PAAm DN gels

The anisotropic structure of the squid/PAAm-6 DN gel resulted in anisotropic mechanical properties. The squid/PAAm-6 DN gels and relevant samples were stretched along the L- and C-axes (Fig. 2a). Figure 2b, c shows the uniaxial stress–strain curves of the PAAm gel, the pure (untreated) squid, the heated squid, and the squid/PAAm-6 DN gel. In this experiment, the pure squid was the untreated squid just after defrosting, and the heated squid was the specimen heated at 65 °C for 12 h without immersion in the monomer solution. The isotropic PAAm gel was soft and stretchable with a fracture strain reaching 7. In contrast, the tensile properties of both the pure and heated squids were brittle, stiff, and anisotropic. The fracture strains of both squid samples remained less than 1, indicating their brittleness. The Young's modulus values of both squids were larger than those of the PAAm gel. The modulus of the pure squid along the L-axis was larger than that along the C-axis; however, this tendency reversed due to the heat treatment. Regardless of the differences in physical properties, both the squid (untreated and heated) and PAAm gels were mechanically weak, exhibiting fracture stresses of less than 0.1 MPa. However, the mechanical properties of the squid/PAAm-6 DN gel remarkably improved relative to those of the parent materials while maintaining the anisotropy. The maximum stresses of the DN gel were more than 0.1 MPa for both axes, which were significantly higher than those of the squid specimens (Fig. 2d). The fracture strain of the DN gel along the L-axis was approximately 2; it could be stretched to a strain of approximately 5 along the C-axis (Fig. 2e). In addition, at a strain of approximately 1, strain hardening was observed when stretched along the L-axis; softening was observed when stretched along the C-axis (Fig. 2b). Notably, the squid specimens were cut from the downside of the mantle, whereas the effects of the cutting position on the mechanical properties of the squid/PAAm DN gel were not significant (Supplementary Fig. 2).

Figure 3a–j shows pictures of the fractured specimens of the squid/PAAm-6 DN gels and the related materials upon uniaxial stretching. The pure squid stretched along both the C- and L-axes exhibited highly ductile fracture with neck formation (Fig. 3a, f). However, the heated squid and the squid/PAAm-6 DN gel showed brittle fracture when stretched along the L-axis (Fig. 3b–e). Moreover, the samples exhibited rough L–T fractured planes when stretched along the C-axis (Fig. 3g–j). We further tried to observe the fractured planes by LV–SEM with high magnification. Because the nonflat fractured planes could not be measured clearly in the low-vacuum mode due to the gradual drying during the observation, we only showed the C–T fractured plane of the heated squid and the squid/PAAm-6 DN gel (Fig. 3k, l). For the heated squid (Fig. 3k), radial muscle fibers oriented along the T-axis were observed, suggesting that the fracture of the heated squid at the C–T plane was caused by the detachment of the radial muscle fibers. However, for the DN gel (Fig. 3i), circular muscle fibers oriented along the C-axis were observed, suggesting the fracture of the DN gel by the detachment of the circular muscle fibers.

We conducted cyclic tensile tests to investigate the origin of the anisotropic mechanical properties of the pure squid and squid/PAAm-6 DN gels. Figure 4a, b

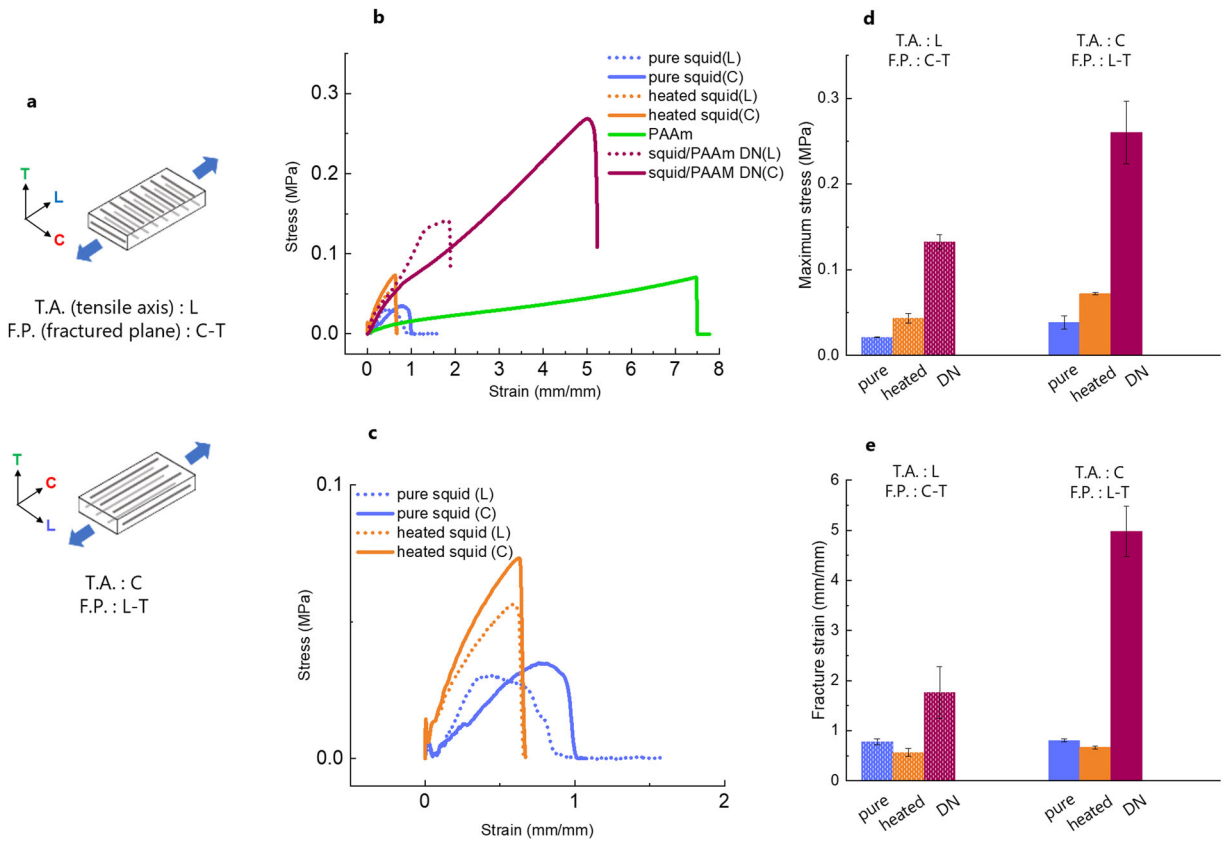

Fig. 2 Squid/PAAm DN gels with enhanced anisotropic tensile properties. a Tensile geometries of the specimen. T. A. and F. P. represent the tensile axis and fractured plane, respectively. **b** Uniaxial tensile stress–strain curves of the pure squid, heated squid, PAAm gel, and squid/PAAm-6 DN gel along the L- or C-axis. Letters in the bracket (L or C) denote the tensile direction. **c** Enlarged graph of (**b**) in the small strain regime (0–2). **d** Maximum stress and **e** fracture strain of the specimens stretched along the L- and C-axes. Data are represented as the mean ± SD with $n = 3$.

shows the cyclic tensile curves of the pure squid along the C- and L-axes, respectively. Almost irreversible mechanical hysteresis and large residual strain characteristics were observed in both axes. Since the mechanical hysteresis of pure squid was independent of the time interval between the adjacent cycles (Supplementary Fig. 3), the mechanical behavior of pure squid was plasto-viscoelastic. Figure 4c, d and Fig. 4e, f show the cyclic curves of the heated squid and squid/PAAm-6 DN gel, respectively, along the C- and L-axes. In both cases, mechanical hysteresis was partly reversible in both axes. Moreover, the occurrence of residual strain in both axes was effectively suppressed.

The following discussion on the anisotropic structure and mechanical properties of the squid/PAAm DN gel was made based on the above mechanical and fracture observations. Because the connective tissue of the squid did not strongly bind muscle fibers to each other, semi-permanent slippage or detachment of the muscle fibers could occur during the deformation of the pure squid[32]. This phenomenon corresponded well to the low fracture stress, highly ductile fracture, and plasto-viscoelastic deformation of the pure squid. By heating squid at 65 °C, the connective tissue was partly denatured, corresponding to the longitudinal shrinkage and lead aggregation of the muscle fibers[36]. Since the squid became more elastic due to aggregation, the heated squid exhibited suppressed residual strain and brittle fracture. However, the aggregated muscle fibers still lacked large deformability. For squid/PAAm DN gels, in addition to the aggregation of the muscle fibers due to thermal polymerization, the introduced PAAm network functioned as a matrix around the muscle fibers. Since PAAm exhibited hydrogen bonding capabilities through the side-chain amide groups, the formation of a robust muscle fiber-gel interface was highly expected[37]. Such a robust fiber-gel interface could enhance the mechanical properties of squid/PAAm DN gels because the strong bonding between the matrix and fibers in composites generally enhanced the strength of the composites[38]. When the squid/PAAm DN gel was stretched along the L-axis, a stretching force was applied between the muscle fibers for

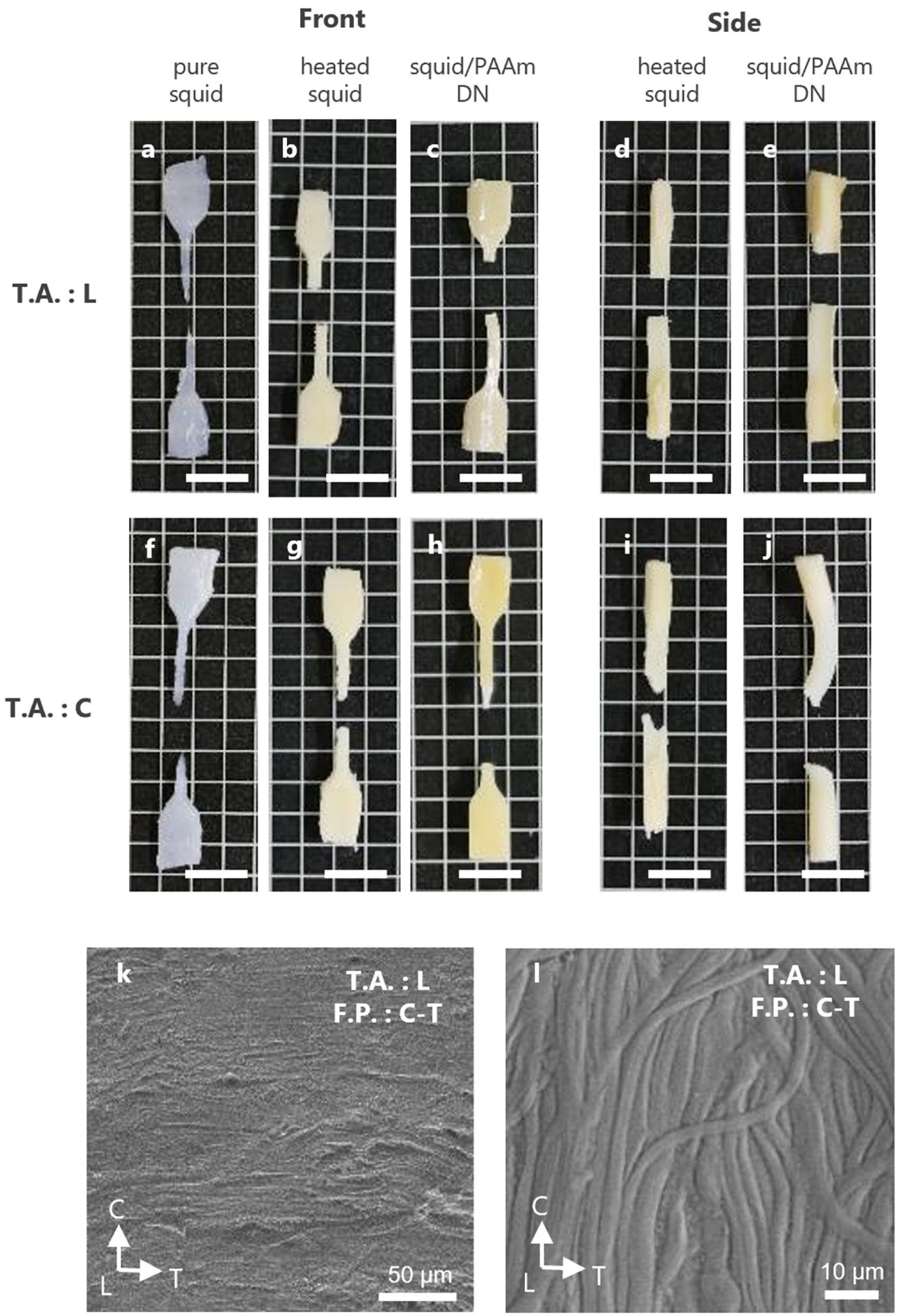

Fig. 3 Different fracture behaviors of the squid/PAAm DN gels along the tensile axis. a–j Photos of the fractured pure squid, heated squid, and squid/PAAm-6 DN gel stretched along the L-axis and C-axis. Scale bars: 1 cm. LV–SEM images of the C–T fractured plane of (**k**) the heated squid and (**l**) the squid/PAAm-6 DN gel.

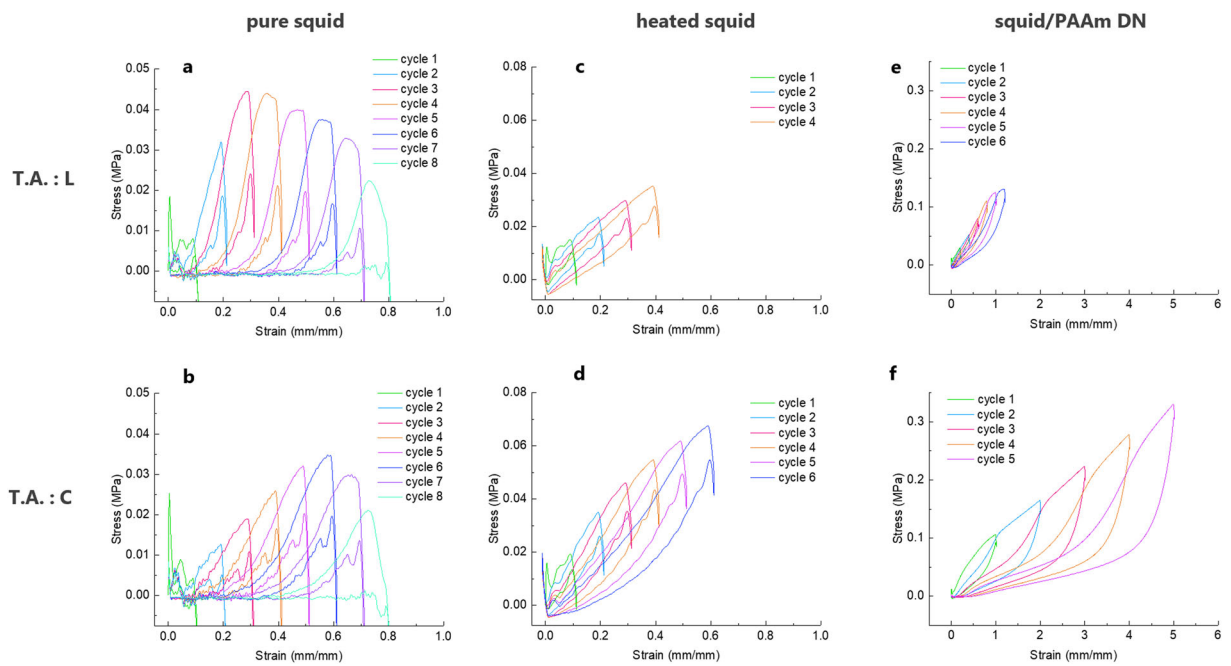

Fig. 4 Cyclic tensile curves. Cyclic tensile curves of the **a, b** pure squid and **c, d** heated squid along the **a**, **c** L- and **b**, **d** C-axes. The spike-like peaks in the graphs are artifacts caused by a mechanical problem. Cyclic tensile curves of the squid/PAAm-6 DN gel along the **e** L-axis and **f** C-axis.

detachment. At this time, the PAAm network confined between the muscle fibers was strongly stretched, accompanied by strain hardening (Fig. 2b). The DN gel was finally fractured by detaching the circular muscle fibers through the rupture of the PAAm network (Fig. 3i). However, when the squid/PAAm DN gel was stretched along the C-axis, the gel between the fibers underwent shear deformation. The gel was largely deformed along the C-axis due to the sliding of the fibers accompanied by strain softening. The rough L–T fracture surface implied that the DN gel was finally broken by the rupture of the circular muscle fiber bundles near the stretching limit of the PAAm matrix.

As discussed above, the mechanical properties of the squid/PAAm DN gel were likely determined by the interplay of the two components through the interaction at the interface. From this viewpoint, the squid/PAAm DN gel could be regarded as a soft composite with squid muscle fibers as fillers.

Anisotropic fracture toughness of the squid/PAAm DN gels

We observed the enhanced anisotropic toughness of the squid/PAAm DN gel using the trouser tear and single-edge notch tests. For the tear test, the initial notch was imposed on the L–T plane (crack propagation along the L-axis) or C–T plane (along the C-axis) of the specimen (Fig. 5a). The tearing energy, T, was estimated as $T = 2F_{ave}/t$ without considering the stretch of the legs, where F_{ave} is the average tearing force and t is the thickness of the gel[34]. The pure squid was tearable along both planes, as shown in Fig. 5b, c; however, tearing along the L–T plane showed a remarkably higher tearing energy of 1400 J m^{-2} relative to that along the C–T plane (200 J m^{-2}). The heated squid and the squid/PAAm DN gels could be torn along the C–T plane (Fig. 5e, g); however, if the tearing test was performed along the L–T plane, the crack immediately bended 90° and propagated along the C–T plane (Fig. 5d, f). This crack bending indicated that the tearing energies of the heated squid and the squid/PAAm DN gels along the L–T plane were significantly higher than those along the C–T plane. Figure 5h shows the tearing energies of the pure squid, the heated squid and the DN gels. Notably, the tearing energy of the heated squid and the DN gel along the L–T plane could not be measured due to crack bending. The tearing energy along the C–T plane significantly increased from 200 (pure squid) to 1400 J m^{-2} by compositing the squid with PAAm.

For the single-edge notch test, the initial notch was imposed on the C–T plane or L–T plane of the rectangular specimen (Fig. 6a). Figure 6b, c shows photographs of the squid/PAAm-6 DN gels subjected to a single-edge notch test, and Fig. 6d shows the load–displacement curves of the notched DN gels. Movies of the single-edge notch test are available as Supplementary Movies 1 and 2. When an initial notch was imposed on the C–T plane and

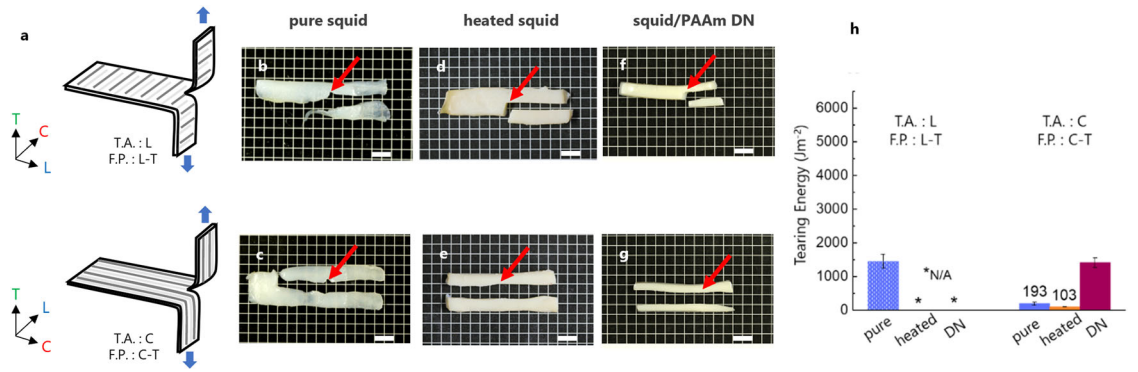

Fig. 5 Tear test results of the squid/PAAm DN gels. a Geometries of specimens for the trouser tear test. **b–g** Photos of specimens after the tear test; **b, c** pure squid torn along the (**a**) L-axis and (**b**) C-axis, heated squid torn along the **d** L-axis and **e** C-axis, and squid/PAAm-6 DN gels torn along the **f** L-axis and **g** C-axis. Red arrows indicate the starting point of tearing. Scale bars: 1 cm. **h** Tearing energies of the pure squid, heated squid, and squid/PAAm-6 DN gels torn along the L-axis or C-axis. Note that the tearing energies of the heated squid and DN gel along the L-axis were unmeasurable due to crack bending. Data are represented as the mean ± SD with $n = 3$.

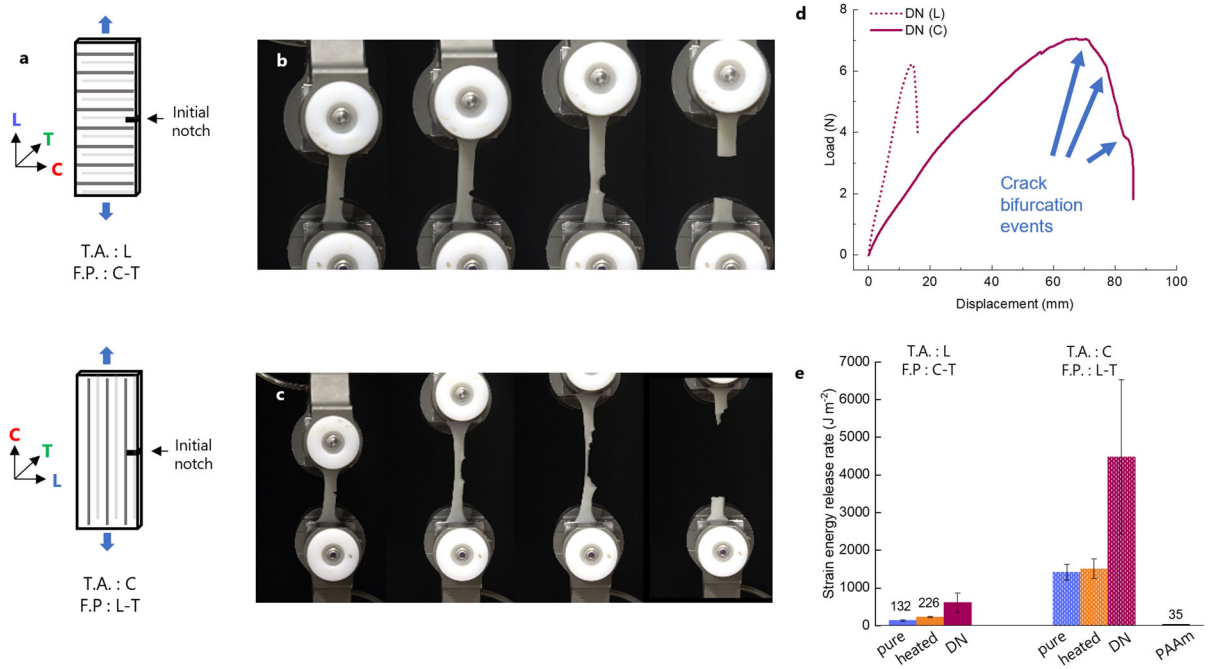

Fig. 6 Single edge-notch test results of the squid/PAAm DN gels. a Geometries of a specimen for the single-edge notch test. **b, c** Time-lapse photos of the single-edge notch test of the squid/PAAm-6 DN gel along the **b** L- and **c** C-axes. **d** Load–displacement curves of the single-edge notch test of the squid/PAAm-6 DN gel. Blue arrows indicate crack bifurcation events. **e** Strain energy release rate (G) of the pure squid, heated squid, PAAm gel, and squid/PAAm DN-6 gel. Data are represented as the mean ± SD with $n = 3$. The large errors could be attributed to the sample-to-sample variation.

stretched along the L-axis, corresponding to a fracture parallel to the circular muscle, the straight propagation of the crack after a small extension was observed. However, when the notch was imposed on the L–T plane and stretched along the C-axis, corresponding to a fracture perpendicular to the circular muscle, the crack did not propagate simply perpendicularly to the circular muscle; instead, the crack sometimes branched in a direction parallel to the circular muscle. This phenomenon resulted in multistep crack propagation. Such bifurcation and refraction of cracks are often observed during the fracture of anisotropic materials[39]. Furthermore, as shown in Fig. 6c, a large displacement was required for the complete crack propagation to the DN gel along the L-axis.

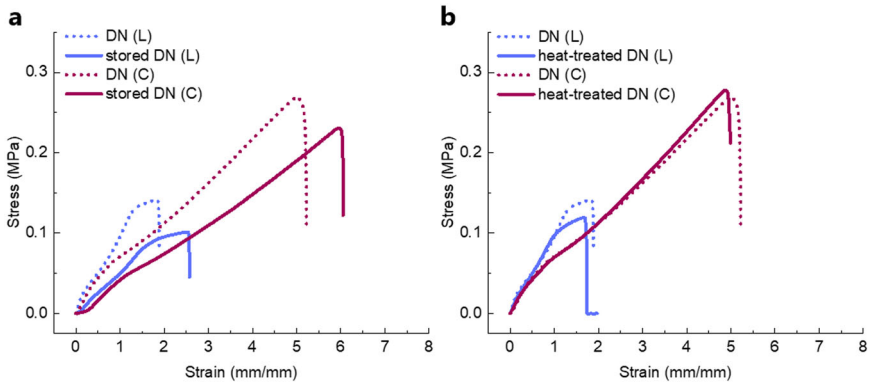

Fig. 7 Degradation resistance of the squid/PAAm DN gels. a Uniaxial tensile stress–strain curves of the fresh squid/PAAm-6 DN gel (DN) and squid/PAAm-6 DN gel after 2 months of storage (stored DN). **b** Uniaxial stress–strain curves of the fresh squid/PAAm-6 DN gel and the squid/PAAm-6 DN gel after heat treatment (heat-treated DN).

This phenomenon indicated that the fracture resistance of the squid/PAAm DN gel along the L–T plane was significantly larger than that along the C–T plane; these findings were consistent with the tear test results. Figure 6d shows a summary of the strain energy release rate, G, of the squid/PAAm DN gels and their parents. The strain energy release rate is an index of the toughness values of materials; it was calculated using the formula $G = \frac{6}{\sqrt{\lambda_b}} W(\lambda_b)c$, where λ_b is the fracture strain of the notched samples and $W(\lambda_b)$ is the area under the stress–strain curve of the corresponding unnotched samples at the strain of λ_b [34]. The G value of the PAAm gel was as low as 35 J m^{-2}. The pure squid and heated squid exhibited strongly anisotropic G values; the G value along the C–T plane was approximately 100 J m^{-2}, whereas that along the L–T plane was approximately 1500 J m^{-2}; these findings were consistent with the tearing test results. However, the G values of the squid/PAAm-6 DN gel along the C–T plane were approximately 500 J m^{-2}, which was significantly higher than those of the pure squid and heated squid. Moreover, the measured G of the DN gel along the L–T plane reached 4000 J m^{-2}, which was comparable to the maximum fracture toughness of DN gels reported until now[40]. Note that we set the initial crack length c as 2 mm, while a smaller c was preferable for correct measurements[34]. If we used $c = 1$ mm for the single-edge notch test of the DN gel, the specimen ruptured near the gripper without crack propagation from the initial crack. This phenomenon suggested that the true G of the squid/PAAm-6 DN gel was remarkably greater than the measured G.

The two types of fracture tests revealed the anisotropic enhanced fracture toughness values of the squid/PAAm DN gels. The toughness of the DN gel along the L–T plane was remarkably larger than that along the C–T plane because the fracture along the L–T plane required the rupturing of the muscle fiber; fracture along the C–T plane only required the peeling of the muscle fiber interface. Such anisotropic toughness of the squid/PAAm DN gels was demonstrated by the notch introduction test (Supplementary Movies 3 and 4). When a DN gel with a suspended weight was notched along the C-axis, the gel immediately ruptured. However, when the gel was notched along the L-axis, no crack propagation was observed. The presence of the PAAm network enhanced the toughness of squids, probably because the densely introduced PAAm network bound the muscle fiber bundles strongly. This hypothesis was supported by the fact that the toughness of the squid/PAAm DN gel increased with increasing PAAm concentration (Supplementary Fig. 4).

Degradation resistance

Pure squid gradually degraded after long-term storage or heat treatment[31,32]. Therefore, whether the obtained squid/PAAm-6 DN gel would degrade with time or by heating was investigated. Figure 7a shows the tensile stress–strain curves of the squid/PAAm-6 DN gel left for two months at 4 °C. The DN gel maintained its high strength after two months of storage, while there was little deterioration in the physical properties. Figure 7b shows the stress–strain curves of the squid/PAAm-6 DN gel heated at 90 °C for 1 h. In this case, no significant deterioration was observed (Supplementary Fig. 5). The mechanical deterioration of pure squid was mainly caused by the denaturation of connective tissue that bound the muscle fibers. In squid/PAAm DN gels, the stable PAAm matrix was substituted for connective tissue. This phenomenon could explain why the significant mechanical deterioration of the squid/PAAm DN gels due to heat or long-term storage was not observed.

Conclusions

We successfully synthesized a tough and anisotropic squid/PAAm DN hydrogel using the squid mantle as a primary network. The DN gel was prepared using a low-energy process by leaving the precursor at 65 °C for 10 h. The tensile properties of the squid/PAAm DN gels were significantly enhanced relative to those of untreated squid while maintaining the anisotropy from the squid mantle muscle. In addition, a squid/PAAm DN gel could serve as a material with remarkable fracture resistance, where cracks would be less likely to propagate across muscle fibers. The introduced PAAm could function as an artificial connective tissue that strongly bound to the muscle fibers of squid and provided elasticity and stability to the material. To date, we do not have evidence of interactions between the squid muscle fibers and PAAm. Thus, the effects of the gel−fiber interaction on the mechanical and fracture properties of the materials were not clear, which was a limitation of this study that should be investigated in the future.

The squid/PAAm DN gel would be potentially useful as load-bearing artificial fibrous tissues, such as artificial ligaments and tendons. The basic criteria of artificial fibrous tissues were biocompatibility, high fracture resistance, and high elastic modulus. The squid/PAAm DN gel was potentially biocompatible after removing residual unreacted monomers (Supplementary Fig. 6), and it exhibited excellent fracture toughness. Unfortunately, the elastic modulus was not sufficient at this point for this purpose and had to be improved by modifying the compositions of the two components.

As shown by the squid/PAAm DN gels in this paper, the preparation of natural/synthetic DN gels was an effective and general method for producing tough DN gels with outstanding functions derived from the anisotropy characteristics of biological products. Anisotropy and related mechanical functions were controllable by choosing natural products for the primary network. The study of natural/synthetic DN gels would aid the development of anisotropic gels with elaborate structures and functions for more practical applications.

Acknowledgements

This research was supported by JSPS KAKENHI grant numbers 17H06144 and 22H04968. The Institute for Chemical Reaction Design and Discovery (WPI-ICReDD) was established by the World Premier International Research Initiative (WPI), MEXT, Japan.

Author details

[1]Graduate School of Life Science, Hokkaido University, Sapporo, Hokkaido 001-0021, Japan. [2]Faculty of Advanced Life Science, Hokkaido University, Sapporo, Hokkaido 001-0021, Japan. [3]Institute for Chemical Reaction Design and Discovery (WPI-ICReDD), Hokkaido University, Sapporo, Hokkaido 001-0021, Japan

Conflict of interest

The authors declare no competing interests.

Supplementary information The online version contains supplementary material available at https://doi.org/10.1038/s41427-022-00454-9.

Received: 28 June 2022 Revised: 8 November 2022 Accepted: 11 November 2022.
Published online: 20 January 2023

References

1. Liu, Z., Zhang, Z. & Ritchie, R. O. Structural orientation and anisotropy in biological materials: functional designs and mechanics. *Adv. Funct. Mater.* **30**, 1–17 (2020).
2. Fung, Y. C. *Biomechanics: Mechanical Properties of Living Tissues* 2nd ed. (Springer, 1993).
3. Sun, J. & Bhushan, B. Hierarchical structure and mechanical properties of nacre: a review. *RSC Adv.* **2**, 7617–7632 (2012).
4. Holbrook, N. N. & Zwieniecki, M. A. *Vascular Transport in Plants* (Elsevier, 2011).
5. Erol, O., Pantula, A., Liu, W. & Gracias, D. H. Transformer hydrogels: a review. *Adv. Mater. Technol.* **4**, 1–27 (2019).
6. Zhao, X. Multi-scale multi-mechanism design of tough hydrogels: building dissipation into stretchy networks. *Soft Matter* **10**, 672–687 (2014).
7. Gong, J. P., Katsuyama, Y., Kurokawa, T. & Osada, Y. Double-network hydrogels with extremely high mechanical strength. *Adv. Mater.* **15**, 1155–1158 (2003).
8. Gong, J. P. Why are double network hydrogels so tough? *Soft Matter* **6**, 2583–2590 (2010).
9. Ito, K. Novel cross-linking concept of polymer network: synthesis, structure, and properties of slide-ring gels with freely movable junctions. *Polym. J.* **39**, 489–499 (2007).
10. Haraguchi, K. Synthesis and properties of soft nanocomposite materials with novel organic/inorganic network structures. *Polym. J.* **43**, 223–241 (2011).
11. Li, J. & Mooney, D. J. Designing hydrogels for controlled drug delivery. *Nat. Rev. Mater.* **1**, 16071 (2016).
12. Sano, K., Ishida, Y. & Aida, T. Synthesis of anisotropic hydrogels and their applications. *Angew. Chem. Int. Ed.* **57**, 2532–2543 (2018).
13. Yusuf, Y. et al. Swelling dynamics of liquid crystal elastomers swollen with low molecular weight liquid crystals. *Phys. Rev. E* **69**, 1–9 (2004).
14. Haque, M. A., Kamita, G., Kurokawa, T., Tsujii, K. & Gong, J. P. Unidirectional alignment of lamellar bilayer in hydrogel: one-dimensional swelling, anisotropic modulus, and stress/strain tunable structural color. *Adv. Mater.* **22**, 5110–5114 (2010).
15. Dobashi, T., Nobe, M., Yoshihara, H., Yamamoto, T. & Konno, A. Liquid crystalline gel with refractive index gradient of curdlan. *Langmuir* **20**, 6530–6534 (2004).
16. Guo, Y. Z. et al. Facile preparation of cellulose hydrogel with Achilles tendon-like super strength through aligning hierarchical fibrous structure. *Chem. Eng. J.* **428**, 132040 (2022).
17. Wu, J., Zhao, Q., Sun, J. & Zhou, Q. Preparation of poly(ethylene glycol) aligned porous cryogels using a unidirectional freezing technique. *Soft Matter* **8**, 3620–3626 (2012).
18. Kim, Y. S. et al. Thermoresponsive actuation enabled by permittivity switching in an electrostatically anisotropic hydrogel. *Nat. Mater.* **14**, 1002–1007 (2015).
19. Sydney Gladman, A., Matsumoto, E. A., Nuzzo, R. G., Mahadevan, L. & Lewis, J. A. Biomimetic 4D printing. *Nat. Mater.* **15**, 413–418 (2016).
20. Weng, L., Gouldstone, A., Wu, Y. & Chen, W. Mechanically strong double network photocrosslinked hydrogels from *N,N*-dimethylacrylamide and glycidyl methacrylated hyaluronan. *Biomaterials* **29**, 2153–2163 (2008).
21. Hagiwara, Y., Putra, A., Kakugo, A., Furukawa, H. & Gong, J. P. Ligament-like tough double-network hydrogel based on bacterial cellulose. *Cellulose* **17**, 93–101 (2010).
22. Yang, W., Furukawa, H. & Gong, J. P. Highly extensible double-network gels with self-assembling anisotropic structure. *Adv. Mater.* **20**, 4499–4503 (2008).

23. Wu, Z. L. et al. Strain-induced molecular reorientation and birefringence reversion of a robust, anisotropic double-network hydrogel. *Macromolecules* **44**, 3542–3547 (2011).
24. Wang, X., Wang, H. & Brown, H. R. Jellyfish gel and its hybrid hydrogels with high mechanical strength. *Soft Matter* **7**, 211–219 (2011).
25. Ding, X. et al. Tough and conductive polymer hydrogel based on double network for photo-curing 3D printing. *Mater. Res. Express* **7**, 055304 (2020).
26. Ward, D. V. Locomotory function of the squid mantle. *J. Zool.* **167**, 487–499 (1972).
27. Macgillivray, P. S., Anderson, E. J., Wright, G. M. & Demont, M. E. Structure and mechanics of the squid mantle. *J. Exp. Biol.* **202**, 683–695 (1999).
28. Moon, T. W. & Hulbert, W. C. The ultrastructure of the mantle musculature of the squid Symplectoteuthis oualaniensis. *Comp. Biochem. Physiol. B Biochem.* **52**, 145–149 (1975).
29. Bone, Q., Pulsford, A. & Chubb, A. D. Squid mantle muscle. *J. Mar. Biol. Assoc.* **61**, 327–342 (1981).
30. Kuo, J.-D., Peleg, M. & Hultin, H. O. Tensile characteristics of squid mantle. *J. Food Sci.* **55**, 369–371 (1990).
31. Kuo, J.-D., Hultin, H. O., Peleg, M. & Atallah, M. T. Effects of heating and postmortem aging on physical properties of squid mantle. *J. Food Process. Preserv.* **15**, 125–133 (1991).
32. Kugino, M. & Kugino, K. Microstructural and rheological properties of cooked squid mantle. *J. Food Sci.* **59**, 792–796 (1994).
33. Kiyama, R. et al. Nanoscale TEM imaging of hydrogel network architecture. *Adv. Mater.* https://doi.org/10.1002/adma.202208902 (2022), in press.
34. Long, R. & Hui, C.-Y. Fracture toughness of hydrogels: measurement and interpretation. *Soft Matter* **12**, 8069–8086 (2016).
35. Stanley, D. W. & Smith, A. K. Microstructure of squid muscle and its influence on texture. *Can. Inst. Food Sci. Technol. J.* **17**, 209–213 (1984).
36. Ando, M. Correspondence of collagen on the heat-induced softening of frozen-thawed cuttlefish sepia officinalis mantle. *J. Home Econ. Jpn.* **48**, 315–321 (1997).
37. Paduka, E., Rottreau, T., Evans, R., Topham, P. D. & Greenall, M. J. Hydrogen bonding aggregation in acrylamide: theory and experiment. *Macromolecules* **51**, 7032–7043 (2018).
38. Karger-Kocsis, J., Mahmood, H. & Pegoretti, A. Recent advances in fibre/matrix interphase engineering for polymer composites. *Prog. Mater. Sci.* **73**, 1–43 (2015).
39. Wilkerson, R. P. et al. A study of size effects in bioinspired, "nacre-like", metal-compliant-phase (nickel-alumina) coextruded ceramics. *Acta Mater.* **148**, 147–155 (2018).
40. Sun, J.-Y. et al. Highly stretchable and tough hydrogels. *Nature* **489**, 133–136 (2012).